

This discussion paper is/has been under review for the journal Atmospheric Chemistry and Physics (ACP). Please refer to the corresponding final paper in ACP if available.

Interaction of chemical and transport processes during the formation of the Arctic stratospheric polar vortex

D. Blessmann, I. Wohltmann, R. Lehmann, and M. Rex

Alfred Wegener Institute for Polar and Marine Research, Potsdam, Germany

Received: 10 May 2011 – Accepted: 24 May 2011 – Published: 8 December 2011

Correspondence to: M. Rex (markus.rex@awi.de)

Published by Copernicus Publications on behalf of the European Geosciences Union.

Chemical and transport processes during vortex formation

D. Blessmann et al.

[Title Page](#)

[Abstract](#)

[Introduction](#)

[Conclusions](#)

[References](#)

[Tables](#)

[Figures](#)

[⏪](#)

[⏩](#)

[◀](#)

[▶](#)

[Back](#)

[Close](#)

[Full Screen / Esc](#)

[Printer-friendly Version](#)

[Interactive Discussion](#)



Abstract

Dynamical processes during the formation phase of the Arctic polar vortex can introduce considerable interannual variability in the amount of ozone that is incorporated into the vortex. Chemistry in autumn and early winter tends to remove part of that variability because ozone relaxes towards equilibrium. As a quantitative measure of how relevant variable dynamical processes during vortex formation are for the winter ozone abundances above the Arctic we analyze which fraction of an ozone anomaly induced dynamically during vortex formation persists until mid-winter. The work is based on the Lagrangian Chemistry Transport Model ATLAS. Model runs for the winter 1999–2000 are used to assess the fate of an ozone anomaly artificially introduced during the vortex formation phase. From these runs we get detailed information about the persistence of the induced ozone variability over time, height and latitude. Induced ozone variability survives longer inside the polar vortex compared to outside. At 540 K inside the polar vortex half of the initial perturbation survives until mid-winter (3 January) with a rapid fall off towards higher levels, mainly due to NO_x induced chemistry. At 660 K 10 % of the initial perturbation survives. Above 750 K the signal falls to values below 0.5 %. Hence, dynamically induced ozone variability from the vortex formation phase can not significantly contribute to mid-winter variability at levels above 750 K. At lower levels increasingly larger fractions of the initial perturbation survive, reaching 90 % at 450 K. In this vertical range dynamical processes during the vortex formation phase are crucial for the ozone abundance in mid-winter.

1 Introduction

Stratospheric ozone plays an important role in the climate system. Due to its absorption of harmful UV-B radiation from the sun stratospheric ozone is important for life on earth. Absorption of UV and visible light by ozone is the main source of heat in the stratosphere. Hence changes in the ozone layer have a direct impact not only on

ACPD

11, 32283–32300, 2011

Chemical and transport processes during vortex formation

D. Blessmann et al.

Title Page

Abstract

Introduction

Conclusions

References

Tables

Figures

⏪

⏩

◀

▶

Back

Close

Full Screen / Esc

Printer-friendly Version

Interactive Discussion



biological systems at the ground but also on the radiative properties of the atmosphere, its thermal structure and hence the global climate.

The ozone layer in the Arctic stratosphere shows a large interannual variability, particularly in spring. Variability in spring is mainly caused by interannual changes in chemical loss, transport by the Brewer-Dobson circulation and mixing during winter, where variability in the chemical loss explains about half of the spring variability of ozone (Tegtmeier et al., 2008). The variability in spring persists several months and slowly decays to the chemically determined equilibrium by the end of the summer (Fioletov and Shepherd, 2003).

Here we focus on the variability which is then newly introduced by transport processes during the formation of the polar vortex in autumn. We are going to investigate on which timescales this variability is conserved or decays because of chemical processes in the subsequent weeks and months (early winter). The results will strongly depend on the altitude if the atmosphere.

How this early winter ozone variability might be related to total ozone later in the winter was investigated by Kawa et al. (2005) and Sinnhuber et al. (2006). They found a correlation between the early winter (November) ozone abundance and late winter (March) total ozone. However, the causes of this correlation remain unclear.

At the end of summer, just before the polar vortex forms, the interannual variability in the ozone abundance is low throughout the Arctic stratosphere. The following variability of polar ozone in early winter is related to wave activity and mixing from lower latitudes (Rosenfield and Schoeberl, 2001; Kawa et al., 2003).

In the Arctic stratosphere the circulation in summer is characterized by slow easterly motion, preventing the vertical propagation of planetary scale waves from their source regions in the troposphere into the stratosphere (Charney and Drazin, 1961). But after autumnal equinox thermal emission leads to subsidence of air over the polar region and to a reversal of the circulation, westerly winds and eventually to the formation of the polar vortex. Then the strong westerlies surrounding the polar vortex again prevent the vertical propagation of planetary waves and suppress meridional mixing. But during

Chemical and transport processes during vortex formation

D. Blessmann et al.

Title Page

Abstract

Introduction

Conclusions

References

Tables

Figures



Back

Close

Full Screen / Esc

Printer-friendly Version

Interactive Discussion



Chemical and transport processes during vortex formation

D. Blessmann et al.

[Title Page](#)[Abstract](#)[Introduction](#)[Conclusions](#)[References](#)[Tables](#)[Figures](#)[⏪](#)[⏩](#)[◀](#)[▶](#)[Back](#)[Close](#)[Full Screen / Esc](#)[Printer-friendly Version](#)[Interactive Discussion](#)

the period of weak westerlies during the vortex formation period waves can propagate freely into the stratosphere and meridional mixing can be strong. The degree to which this effect transports low latitude air and ozone mixing ratios into the Arctic depends on the level of wave activity in the troposphere during this brief sensitive period. Since chemical processes during summer lead to a strong meridional gradient in the ozone field, the variable degree of meridional mixing introduces pronounced variability in the ozone abundance at high latitudes that are then enclosed by the polar vortex.

The variability in ozone levels introduced by this (or any other potential process) during vortex formation tends to decay during the following weeks and months due to relaxation of ozone towards its chemically determined equilibrium. We analyse the fraction of the variability that survives the interaction between transport and chemical processing in autumn. Only this fraction can contribute to the interannual variability of ozone abundances inside the polar vortex in mid-winter. The chemical processing and relaxation towards equilibrium occurs in competition with the decrease in solar insolation which eventually suppresses further chemical conversion of ozone such that the degree of variability remaining at that time is conserved until spring. This study uses a Lagrangian model of chemistry, transport and mixing to quantify how long an initial perturbation of ozone in late summer/early autumn survives the chemical processing and at which altitudes and latitudes it potentially contributes to the spring variability of ozone.

2 Model

The global Chemistry Transport Model ATLAS was used to investigate the interaction of chemistry and transport in the period of polar vortex formation and its further influence on ozone distribution all through winter. In the following subsections short descriptions of the model and the model runs are given.

2.1 Model description

ATLAS is a global Chemistry and Transport Model with detailed stratospheric chemistry and a Lagrangian (trajectory-based) transport and mixing scheme (Wohltmann and Rex, 2009; Wohltmann et al., 2010). Lagrangian models have several advantages over conventional Eulerian models, in particular no spurious numerical diffusion and a more realistic transport of chemical species.

The chemistry module comprises 46 active species and 171 reactions. These include 42 photolysis reactions, 122 gas phase reactions and 7 heterogeneous reactions on background sulfate aerosol and various Polar Stratospheric Cloud (PSC) particles formed according to Carslaw et al. (1995). The rate constants are taken from the recommendations in the JPL 2006 catalogue and its 2009 update (Sander et al., 2006, 2009) with the exception of the ClOOCl photolysis cross sections, which are taken from Burkholder et al. (1990), similar to Papanastasiou et al. (2009).

The model contains a particle-based denitrification module based on the DLAPSE model of Carslaw et al. (2002). Further details on the model's chemistry and denitrification and the validation of these modules can be found in Wohltmann et al. (2010).

2.2 Model runs

This study is based on two model runs, a reference run with an unmodified ozone field and a perturbation run. Both runs simulate the period 1 July 1999 to 31 March 2000. In the perturbation run the ozone field is artificially increased by 30 % on 16 September 1999. The purpose of perturbing ozone during polar vortex formation is to investigate how long and where the ozone perturbation survives and how strongly it is damped by chemistry. The perturbation simulates the effect of interannual variability in high latitude ozone during vortex formation. Obviously such perturbations survive longer in regions of longer ozone lifetimes, i.e. at higher latitudes and lower altitudes. The goal of this study is to quantitatively assess to which extent and where autumnal ozone variability can survive chemical processing until ozone becomes long lived in mid-winter.

Chemical and transport processes during vortex formation

D. Blessmann et al.

[Title Page](#)[Abstract](#)[Introduction](#)[Conclusions](#)[References](#)[Tables](#)[Figures](#)[⏪](#)[⏩](#)[◀](#)[▶](#)[Back](#)[Close](#)[Full Screen / Esc](#)[Printer-friendly Version](#)[Interactive Discussion](#)

Chemical and transport processes during vortex formation

D. Blessmann et al.

[Title Page](#)[Abstract](#)[Introduction](#)[Conclusions](#)[References](#)[Tables](#)[Figures](#)[⏪](#)[⏩](#)[◀](#)[▶](#)[Back](#)[Close](#)[Full Screen / Esc](#)[Printer-friendly Version](#)[Interactive Discussion](#)

Chemical species are initialised on 1 August, after a spin up period for the model's transport scheme in July. Initial water vapor (H_2O), methane (CH_4), ozone (O_3), nitrogen dioxide (NO_2 , as a proxy for NO_x) and hydrochloride acid (HCl) are bi-monthly means of August and September 1999 based on measurements of the HALOE solar occultation instrument onboard the Upper Atmosphere Research Satellite (UARS) as function of equivalent latitude and pressure (Grooß and Russell III, 2005). Nitric acid (HNO_3) and carbon monoxide (CO) are initialised with a climatology based on data of the ACE FTS interferometer onboard the SCISAT-1 satellite. N_2O is deduced from a $\text{N}_2\text{O}-\text{CH}_4$ tracer-tracer relationship derived from ER-2 and Triple balloon data (Grooß and Russell III, 2005). The initial values of ClONO_2 are the difference between HCl and Cl_y , which was first calculated from a Cl_y-CH_4 relationship from ER-2 and Triple balloon data (Grooß et al., 2002). The initial Br_y is derived from a Br_y-CH_4 relationship (Grooß et al., 2002) and assumed to be in the form of BrONO_2 . Additionally, in order to achieve an agreement with Differential Optical Absorption Spectroscopy (DOAS) measurements of BrO (Dorf et al., 2008), Br_y is scaled by a constant factor to give maximum values of 19.9 ppt. CFCs and related species are initialised as in Wohltmann et al. (2010).

We have based our model runs on ERA Interim reanalysis data (Simmons et al., 2006, 2007) from the Center for Medium Range Weather Forecast (ECMWF) with a horizontal resolution of $2^\circ \times 2^\circ$ and 60 levels with an approximate vertical resolution of 1.5 km in the stratosphere. The meteorological fields are given every 6 hours. The trajectories are calculated with a 30 min time step. The model runs are carried out with an approximate horizontal resolution of 150 km in a vertical domain from 350 K to 1900 K. The Lyapunov exponent, which adjusts the mixing strength, is set to 4 day^{-1} (Wohltmann and Rex, 2009). As vertical coordinate we used hybrid pressure/potential temperature levels, which are in good approximation a potential temperature coordinate in the stratosphere. The vertical motion is driven by ERA Interim's diabatic heating rates. A validation of ATLAS transport properties was presented by Wohltmann and Rex (2009).

A passive ozone tracer is initialised on 1 August identical to the model's ozone field. In the following, this tracer is only affected by transport and mixing and not by chemistry. The difference between the model's active ozone and this passive ozone tracer is a measure for the chemically induced ozone change.

3 Results

In Fig. 1, we show results of the unperturbed run as reference. Figure 1a shows the time evolution of ozone and Fig. 1b the chemical loss of ozone, both averaged over 65–90°N equivalent latitude. Generally ozone mixing ratios increase with altitude (or potential temperature) and larger mixing ratios subside during the winter, leading to an increase of ozone on fixed potential temperature levels in the lower stratosphere below approximately 575 K (Fig. 1a). In the middle stratosphere the increase in ozone due to subsidence is modified by chemical loss. Air reduced in ozone propagates downward to the lower stratosphere during autumn (Fig. 1b). This natural loss of ozone explains the observed decrease in ozone above 600 K during autumn (Fig. 1a) and also leads to a flattening of vertical gradient between 575 and 950 K potential temperature level (as also observed by Kawa et al., 2003).

The chemically induced decrease in ozone at these altitudes in September and October is due to the fact that the equilibrium concentration of ozone drops while the solar zenith angles increase in autumn. Ozone concentrations in late summer are close to the chemical equilibrium, which results from the balance of ozone production (governed by O₂ photolysis) and loss. At these altitudes under polar summer conditions the loss is dominated by chemistry involving NO_x species, which are present at high concentrations since high amounts of NO_y subsided into the polar middle stratosphere during the preceding winter and these are efficiently converted into NO_x during polar day in summer (Toon et al., 1999).

The ozone production via O₂ photolysis requires the presence of UV radiation ($\lambda < 240$ nm) while the efficiency of NO_x catalysed ozone loss is governed by the

Chemical and transport processes during vortex formation

D. Blessmann et al.

Title Page

Abstract

Introduction

Conclusions

References

Tables

Figures

⏪

⏩

◀

▶

Back

Close

Full Screen / Esc

Printer-friendly Version

Interactive Discussion



photolysis frequency of O₃, which photolyses in visible light ($\lambda < 1180$ nm). When solar zenith angles increase in autumn the availability of UV light drops much faster than that of visible light, since the light path through the ozone layer increases, which absorbs UV light but does not attenuate visible light much. Hence ozone production drops earlier than ozone loss and the equilibrium concentration of ozone decreases. At the same time the lifetime of ozone increases and depending on altitude the timescale of the decrease of equilibrium is shorter than the lifetime of ozone and the actual ozone concentrations relax slowly towards the new equilibrium.

Figure 2 is based on the difference between the reference run and the perturbation run and shows the fraction of the initial ozone perturbation that remains at the different altitudes as function of date. This fraction is calculated as:

$$f = 100 \cdot \frac{\left(\frac{O_3^p - O_3}{O_3} \right)}{p} \quad (1)$$

where f is the remaining signal (as function of altitude and time), O_3 is the ozone concentration in the reference run, O_3^p the ozone concentration in the perturbation run and p the initial perturbation (i.e. 30 %).

Figure 2 shows the value of f averaged over the area north of 65 °N equivalent latitude. The signal is completely lost after 1 month above 1200 K and remains nearly constant at values close to 100 % in the lower stratosphere. Between these layers the signal is gradually lost and remains present to variable degrees until mid-winter, when chemistry becomes so slow, that the remaining signal is preserved.

Figure 3 shows the evolution of f on three potential temperature levels (450 K, 575 K, 750 K) through autumn and early winter. While at 450 K potential temperature most of the signal is still present in early January, the initial perturbation has been almost completely removed at 750 K until this time. At 575 K about 20 % of the initial perturbation are still present in mid-winter.

The vertical profile of f on 3 January is shown in Fig. 4. Above 750 K the initial perturbation is reduced to less than 0.5 % by this date. Here the perturbation has

Chemical and transport processes during vortex formation

D. Blessmann et al.

Title Page

Abstract

Introduction

Conclusions

References

Tables

Figures

⏪

⏩

◀

▶

Back

Close

Full Screen / Esc

Printer-friendly Version

Interactive Discussion



essentially been removed from the system and this level is marked by a horizontal line in the figure. Towards the lower stratosphere the signal rises to its maximum around 90 % at 400 K.

The generally expected behaviour that ozone mixing ratios in the lower stratosphere are more sensitive to and have a longer memory for variability induced by transport and mixing is clearly visible. Furthermore the figure shows this general behaviour in a quantitative way and elucidates at which altitudes transport and mixing processes during vortex formation can influence mid-winter ozone mixing ratios inside the polar vortex to which extent.

Due to the variation of ozone lifetime with latitude, the preservation of dynamically induced ozone variability is not only a function of altitude but also of latitude. Hence we show in Fig. 5 the variation of f as function of potential temperature and equivalent latitude on 3 January 2000. For the figure, the ozone field is binned and averaged into 5 degree equivalent latitude bins and 50 K potential temperature bins. At higher (compared to lower) latitudes a larger fraction of the ozone variability, generated dynamically throughout the formation of the polar vortex in autumn and early winter, is preserved until the beginning of January. This is a consequence of the isolation of the polar vortex from lower latitudes (Kawa et al., 2003) in combination with the longer chemical lifetime of ozone at higher latitudes.

4 Conclusions

Due to the ability of planetary waves to propagate deeply into the stratosphere and the still readily available solar radiation the polar vortex formation phase in high latitude autumn is a period of interesting interaction between chemistry, transport and mixing. Variability induced by transport and mixing during this period is damped by chemistry and the degree to which chemistry compensates for dynamically induced variability depends on the complicated interaction between transport and chemical loss of ozone until polar night conditions suppresses further chemical conversion of ozone. We have

Chemical and transport processes during vortex formation

D. Blessmann et al.

Title Page

Abstract

Introduction

Conclusions

References

Tables

Figures

⏪

⏩

◀

▶

Back

Close

Full Screen / Esc

Printer-friendly Version

Interactive Discussion



Chemical and transport processes during vortex formation

D. Blessmann et al.

Title Page

Abstract

Introduction

Conclusions

References

Tables

Figures



Back

Close

Full Screen / Esc

Printer-friendly Version

Interactive Discussion



used ATLAS, a detailed fully Lagrangian CTM, to study the interaction between transport and chemistry during this phase and have quantified which fraction of dynamically induced variability in ozone survives chemical processing until mid-winter, when ozone becomes a long lived species. The Lagrangian model ATLAS reproduces atmospheric mixing better than Eulerian models, which are usually dominated by numerical diffusion. The ATLAS model is therefore well suited to study the processes during the vortex formation phase, when mixing is strong and very relevant for high latitude ozone mixing ratios.

We found that dynamically induced ozone variability during the polar vortex formation phase can have a strong impact on mid-winter ozone mixing ratios inside the polar vortex up to potential temperature levels of about 600 K, where about 20 % of the initial perturbation is still present in mid January. Moderate but still significant impact of dynamically induced ozone variability extends as high as 750 K, where the chemical ozone loss reduces the initial ozone perturbation to 0.5 % at the beginning of January. Above this level ozone concentrations essentially reach equilibrium at any time between the vortex formation and mid-winter, such that dynamically induced ozone anomalies are removed and the memory in ozone to its transport and mixing processes during vortex formation is destroyed.

These results highlight the importance of interaction between chemistry and dynamical processes during the autumnal circulation reversal for mid-winter ozone mixing ratios inside the polar vortex.

Acknowledgements. We thank ECMWF for providing reanalysis data, K. Walker (U. Toronto) for providing ACE FTS data (The Atmospheric Chemistry Experiment (ACE), also known as SCISAT, is a Canadian-led mission mainly supported by the Canadian Space Agency), J.-U. Grooß and J. M. Russell III for providing HALOE data and ER-2 and Triple balloon tracer relationships. Work at AWI was partially supported by the EC project RECONCILE, Grant Agreement no 236365.

References

- Burkholder, J. B., Orlando, J. J., and Howard, C. J., Ultraviolet absorption cross sections of chlorine oxide (Cl_2O_2) between 210 and 410 nm, *J. Phys. Chem.*, 94, 687–695, 1990. 32287
- 5 Carslaw, K. S., Luo, B., and Peter, T.: An analytical expression for the composition of aqueous HNO_3 - H_2SO_4 stratospheric aerosols including gas phase removal of HNO_3 , *Geophys. Res. Lett.*, 22, 1877–1880, 1995. 32287
- Carslaw, K. S., Kettleborough, J. A., Northway, M. J., Davies, S., Gao, R.-S., Fahey, D. W., Baumgardner, D. G., Chipperfield, M. P., and Kleinböhl, A.: A vortex-scale simulation of the growth and sedimentation of large nitric acid hydrate particles, *J. Geophys. Res.*, 107, 8300, doi:10.1029/2001JD000467, 2002. 32287
- 10 Charney, J. G. and Drazin, P. G.: Propagation of Planetary-scale disturbances from the lower into the upper atmosphere, *J. Geophys. Res.*, 66, 83–109, 1961. 32285
- Dorf, M., Butz, A., Camy-Peyret, C., Chipperfield, M. P., Kritten, L., and Pfeilsticker, K.: Bromine in the tropical troposphere and stratosphere as derived from balloon-borne BrO observations, *Atmos. Chem. Phys.*, 8, 7265–7271, doi:10.5194/acp-8-7265-2008, 2008. 32288
- 15 Fioletov, V. E. and Shepherd, T. G.: Seasonal persistence of midlatitude total ozone anomalies, *Geophys. Res. Lett.*, 30(7), doi:10.1029/2002GL016739, 2003. 32285
- Grooß, J.-U., Günther, G., Konopka, P., Müller, R., McKenna, D. S., Stroh, F., Vogel, B., Engel, A., Müller, M., Hoppel, K., Bevilacqua, R., Richard, E., Webster, C. R., Elkins, J. W., Hurst, D. F., Romanschkin, P. A., and Baumgardner, D. G.: Simulation of ozone depletion in spring 2000 with the Chemical Lagrangian Model of the Stratosphere (CLaMS), *J. Geophys. Res.*, 107, 8295, doi:10.1029/2001JD000456, 2002. 32288
- 20 Grooß, J.-U., and Russell III, J. M.: Technical note: A stratospheric climatology for O_3 , H_2O , CH_4 , NO_x , HCl and HF derived from HALOE measurements, *Atmos. Chem. Phys.*, 5, 2797–2807, doi:10.5194/acp-5-2797-2005, 2005. 32288
- 25 Kawa, S. R., Bevilacqua, R. M., Margitan, J. J., Douglass, A. R., Schoeberl, M. R., Hoppel, K. W., and Sen, B.: Interaction between dynamics and chemistry of ozone in the setup phase of the Northern Hemisphere polar vortex, *J. Geophys. Res.*, 108, 8310, doi:10.1029/2001JD001527, 2003. 32285, 32289, 32291
- 30 Kawa, S. R., Newman, P. A., Stolarski, R. S., and Bevilacqua, R. M.: Fall vortex ozone as a predictor of springtime total ozone at high northern latitudes, *Atmos. Chem. Phys.*, 5, 1655–

Chemical and transport processes during vortex formation

D. Blessmann et al.

Title Page

Abstract

Introduction

Conclusions

References

Tables

Figures

◀

▶

◀

▶

Back

Close

Full Screen / Esc

Printer-friendly Version

Interactive Discussion



**Chemical and
transport processes
during vortex
formation**

D. Blessmann et al.

Title Page

Abstract

Introduction

Conclusions

References

Tables

Figures

⏪

⏩

◀

▶

Back

Close

Full Screen / Esc

Printer-friendly Version

Interactive Discussion



1663, doi:10.5194/acp-5-1655-2005, 2005. 32285

Papanastasiou, D. K., Papadimitriou, V. C., Fahey, D. W., and Burkholder, J. B.: UV Absorption Spectrum of the ClO Dimer (Cl_2O_2) between 200 and 420 nm, *J. Phys. Chem.*, 113(49), 13711–13726, doi:10.1021/jp9065345, 2009. 32287

5 Rosenfield, J. E. and Schoeberl, M. R.: On the origin of polar vortex air, *J. Geophys. Res.*, 106/D24, 33485–33497, 2001. 32285

Sander, S. P., Friedl, R. R., Ravishankara, A. R., Golden, D. M., Kolb, C. E., Kurylo, M. J., Molina, M. J., Moortgat, G. K., Finlayson-Pitts, B. J., Wine, P. H., Huie, R. E., and Orkin, V. L., Chemical kinetics and photochemical data for use in atmospheric studies, Evaluation
10 Number 15, JPL Publication 06-2, Jet Propulsion Laboratory, California Institute of Technology, Pasadena, <http://jpldataeval.jpl.nasa.gov>, 2006. 32287

Sander, S. P., Friedl, R. R., Abatt, J., Barker, J. R., Burkholder, J. B., Golden, D. M., Kolb, C. E., Kurylo, M. J., Moortgat, G. K., Wine, P. H., Huie, R. E., and Orkin, V. L., Chemical kinetics and photochemical data for use in atmospheric studies, Evaluation Number 16, JPL
15 Publication 09-31, Jet Propulsion Laboratory, California Institute of Technology, Pasadena, <http://jpldataeval.jpl.nasa.gov>, 2009. 32287

Simmons, A. J., Uppala, S. M., Dee, D., and Kobayashi, S.: ERA-Interim: New ECMWF reanalysis products from 1989 onwards, *ECMWF News Letter*, 110, 25–35, 2006. 32288

Simmons, A. J., Uppala, S. M., and Dee, D.: Update on ERA-Interim, *ECMWF News Letter*,
20 111, 5, 2007. 32288

Sinnhuber, B.-M., von der Gathen, P., Sinnhuber, M., Rex, M., König-Langlo, G., and Oltmans, S. J.: Large decadal scale changes of polar ozone suggest solar influence, *Atmos. Chem. Phys.*, 6, 1835–1841, doi:10.5194/acp-6-1835-2006, 2006. 32285

Tegtmeier, S., Rex, M., Wohltmann, I., and Krüger, K.: Relative importance of dynamical and chemical contributions to Arctic wintertime ozone, *Geophys. Res. Lett.*, 35, L17801,
25 doi:10.1029/2008GL034250, 2008. 32285

Toon, G., Blavier, F. F., Sen, B., Salawitch, R. J., Osterman, G. B., Notholt, J., Rex, M., McElroy, C. T., and Russell III, J. M., Ground-based observations of Arctic ozone loss during spring and summer 1997, *J. Geophys. Res.*, 104, 26497–26510, 1999. 32289

30 Wohltmann, I. and Rex, M.: The Lagrangian chemistry and transport model ATLAS: validation of advective transport and mixing, *Geosci. Model Dev.*, 2, 153–173, doi:10.5194/gmd-2-153-2009, 2009.

Wohltmann, I., Lehmann, R., and Rex, M.: The Lagrangian chemistry and transport model ATLAS: simulation and validation of stratospheric chemistry and ozone loss in the winter 1999/2000, Geosci. Model Dev., 3, 585–601, doi:10.5194/gmd-3-585-2010, 2010. 32287, 32288

5 32287, 32288

32295

ACPD

11, 32283–32300, 2011

**Chemical and
transport processes
during vortex
formation**

D. Blessmann et al.

Title Page

Abstract

Introduction

Conclusions

References

Tables

Figures

⏪

⏩

◀

▶

Back

Close

Full Screen / Esc

Printer-friendly Version

Interactive Discussion



Chemical and transport processes during vortex formation

D. Blessmann et al.

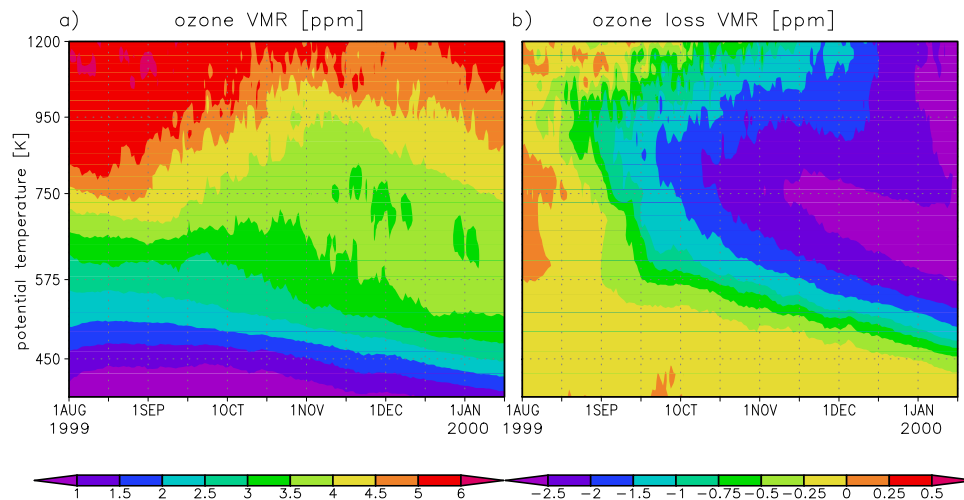


Fig. 1. Time-height-section of area mean ($\geq 65^\circ$ N equivalent latitude) ozone mixing ratios (a) and ozone loss (b).

[Title Page](#)[Abstract](#)[Introduction](#)[Conclusions](#)[References](#)[Tables](#)[Figures](#)[⏪](#)[⏩](#)[◀](#)[▶](#)[Back](#)[Close](#)[Full Screen / Esc](#)[Printer-friendly Version](#)[Interactive Discussion](#)

Chemical and transport processes during vortex formation

D. Blessmann et al.

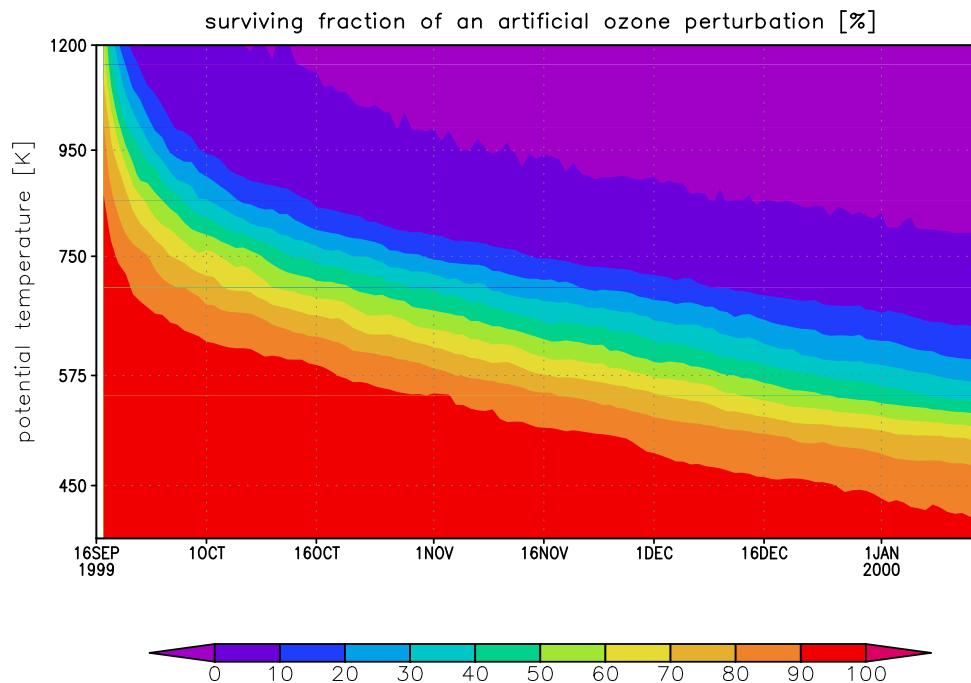


Fig. 2. Time-height-section of surviving fraction of an artificial ozone perturbation on 16 September 1999 after Eq. (1) from 17 September 1999 to 15 January 2000.

Chemical and transport processes during vortex formation

D. Blessmann et al.

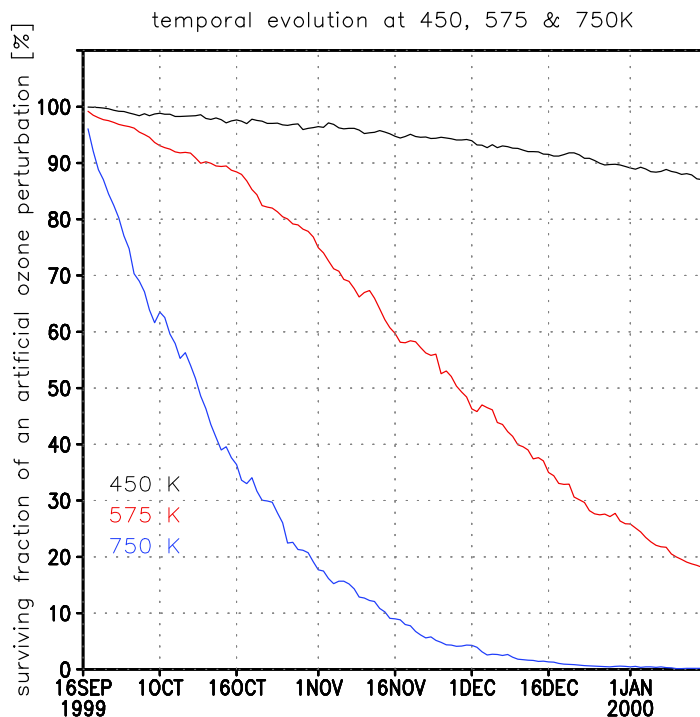


Fig. 3. Temporal evolution of surviving fraction of an artificial ozone perturbation on 16 September 1999 at 450 K (black), 575 K (red) and 750 K (blue) potential temperature levels from 17 September 1999 to 15 January 2000.

[Title Page](#)[Abstract](#)[Introduction](#)[Conclusions](#)[References](#)[Tables](#)[Figures](#)[◀](#)[▶](#)[◀](#)[▶](#)[Back](#)[Close](#)[Full Screen / Esc](#)[Printer-friendly Version](#)[Interactive Discussion](#)

Chemical and transport processes during vortex formation

D. Blessmann et al.

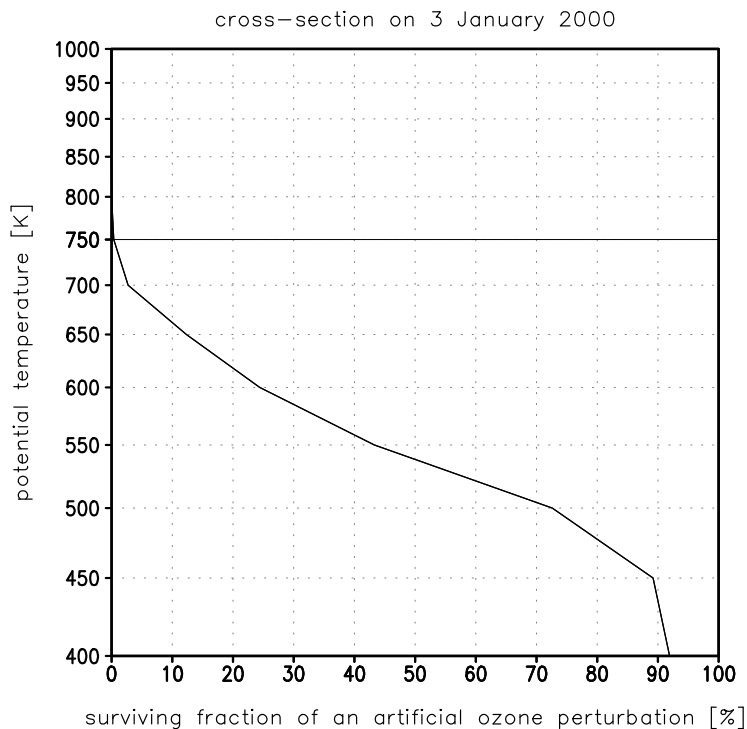


Fig. 4. Vertical profile of surviving fraction of an artificial ozone perturbation on 16 September 1999 on 3 January 2000. Values are smaller than 0.5% above the 750 K potential temperature level (marked by a solid horizontal line).

[Title Page](#)[Abstract](#)[Introduction](#)[Conclusions](#)[References](#)[Tables](#)[Figures](#)[◀](#)[▶](#)[◀](#)[▶](#)[Back](#)[Close](#)[Full Screen / Esc](#)[Printer-friendly Version](#)[Interactive Discussion](#)

Chemical and transport processes during vortex formation

D. Blessmann et al.

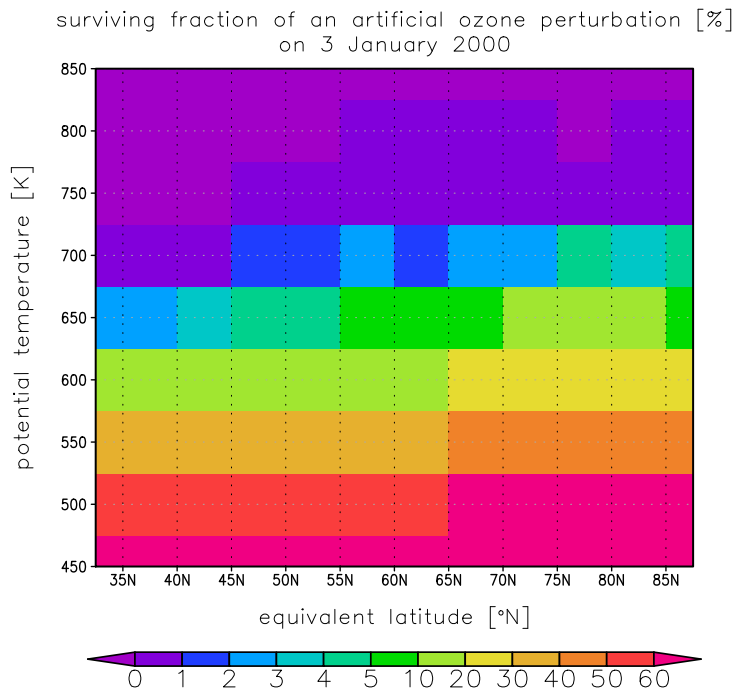


Fig. 5. Surviving fraction of an artificial ozone perturbation on 16 September 1999 is shown against equivalent latitude bins at 5 degree on 3 January 2000.

[Title Page](#)[Abstract](#)[Introduction](#)[Conclusions](#)[References](#)[Tables](#)[Figures](#)[⏪](#)[⏩](#)[◀](#)[▶](#)[Back](#)[Close](#)[Full Screen / Esc](#)[Printer-friendly Version](#)[Interactive Discussion](#)